



Detection of Cancer cells using Feed Planar Antenna

[Pinky Shibu, K. Parasakthi]¹, S.Manikandan²

¹IV BE ECE, PSN College of Engineering and Technology, Tirunelveli.

Email:pinky.shibu.94@gmail.com,parasakthik244@gmail.com

²Asst. Professor, Department of ECE, PSN College of Engineering and Technology, Tirunelveli

Email:sl.manikandan@gmail.com

Abstract-In this paper, design and construction of micro strip feed planar antenna containing both coupling and decoupling structure is proposed. The main advantages of this type of antennas include compact size, ease of integration, reduced weight and lower volume compared with horn. Each antenna element working under the frequency range of 2-16 GHz. To achieve better imaging radar tool a dedicated radar transceiver is used in the proposed system. Segmentation is applied to the decoupled image from transceiver. After, a fresh hybrid artefact removal algorithm for microwave breast imaging applications is presented, which combines the best attributes of two existing algorithms to effectively remove the early-stage artefact. The main concern of this project is to diagnose the harmless tissue at the earliest cancer stage where it is completely curable. The tool is best suited for diagnosis of earliest breast cancer

causing tumour cells having resolution of about 3 mm.

Keyword: Breast cancer, Planar Antenna, Artefact removal, microwave imaging, ultra wideband radar, Microstrip feed skin effect.

I. INTRODUCTION

The dramatic development of wireless communication leads to the development of microwave imaging technique to image human body has been taking place now. As reported in [1], breast cancer is one of the most common tumours among the female population. Since 95% of the cures are possible if they are identified in the earliest stage. At the beginning stage, it could be treated as well and prevented from being the tissue to be malignant. These Microwave integrated devices have its wider applications in the biomedical field.

A fresh hybrid artifact removal algorithm for microwave breast imaging



applications is proposed. The freshness of this study is threefold. First, the authors propose a hybrid artefact removal algorithm that combines the best attributes of the Entropy-based Time Windowing algorithm [1] and Wiener Filter algorithm [2]. It helps to effectively remove the early-stage artefact while preserving the tumour response. Second, the algorithm is evaluated using an anatomically and dielectrically accurate 3-D finite-difference time-domain (FDTD) model (compared to the 2-D homogeneous FDTD model originally used [1]). The FDTD method is based on a discretization of Maxwell's equations in differential form and the fields are solved iteratively in alternating time steps for a selected time period. Third, the hybrid algorithm presented here shows a very clear improvement compared to the original algorithm across a range of appropriate metrics.

II. PLANAR ANTENNAS

Planar antennas are the newest generation of antennas possessing such attractive features such as low profile, low weight, low cost and ease of integration into arrays. These features make them suitable for modern communication systems, particularly in biomedical field. Here in this paper planar antennas are used for designing a new Microwave imaging radar tool. It has valuable usage as a diagnostic tool in the detection of tumour cells at an earlier stage. In this planar antenna layout the strip is designed and feed is through a microstrip line with 50 ohms microstrip line.

III. UWB PATCH ANTENNA

A. Theory

The proposed module consists of two antenna elements which are considered to be the monopole structure. Each antenna element working under a wide bandwidth. It has an operating frequency range of about 2 to 9 GHz. Antenna top layer layout represents the transmitting and receiving radiating patches. The radiation pattern combines both the rectangular and circular patches. The semicircular tapering part gives a better impedance matching all over the bandwidth. The feeding line is chosen to be centre feed. The centre microstrip feed line to these radiating patch provides equal current distribution and provides a good power patch.

Impedance matching should be equal to 50 ohms that certainly provides better input and output transmission and reception. Top layer of the antenna structure represents the coupling structure where the monopoles are placed facing at the same face. To achieve a compact design the monopoles are placed very close to each other which causes mutual coupling between the antennas. These mutual coupling introduces losses and there is a way to avoid these mutual coupling. To avoid this unavoidable mutual coupling a T shaped decoupler is being added to the back of the laminate, which reduces the losses introduced.



Patch element come in various shapes, such as rectangular, square, circular, annual ring, triangular, pentagonal, and square or circular

Frequency	3.3 GHz to 8.5 GHz
Substrate Thickness	1.524
Loss Tangent	0.0027
Feed line (Top Layer)	Length = 9.9mm Width = 1.7mm
Substrate Dielectric constant (ϵ_r)	3.55
Ground Plane	Length = 67 mm Width = 34 mm

with perturbed truncations. Rectangular

Patch is used for linearly polarized applications. Square and circular patches can be excited orthogonally by two feeds to achieve circular polarization. In addition circular polarization can be designed to excite higher order modes for generating different-shaped patterns. One disadvantage of circular and square patch compared to rectangular patch is that they are more susceptible to cross-polarization excitation when used as linearly polarized elements.

B. Antenna Design

Factors deciding the antenna compact design include insertion and isolation factors. For perfect input and output matching to get occur insertion should be high, thereby the insertion loss should be low as possible. Isolation between these monopoles should be high. But isolation loss should be as low as possible. The upper part isolation control

is adapted by the parameters say $wd2$ and $ld2$. Isolation control is adapted by the parameters say $wd1$ and $ld1$ which controls the isolation between the two radiating patches, at the lower part with an operating frequency band of about 2 to 9 GHz.

Four reflector configurations have been commercially developed for the compact design. They are single paraboloid, dual parabolic-cylinder system, dual shaped-reflector, and single parabolic-cylinder systems.

Table 1: Design considerations

C. Antenna Geometry

The Planar antenna geometry is illustrated in the figure 1. The antenna layouts includes the (a) Top layer layout for the coupling structure and (b) Bottom layer layout for decoupling structure with partial ground plane and overall dimensions given. The layout is schematized using software MATLAB. These programs can be used to plot the two-dimensional pattern, both polar and semipolar. The parameters that are needed to calculate include S parameters, reflection coefficients and VWSR. The designing of monopole planar antennas in advanced design systems software includes Laying out the radiating planar patches. Microstrip patch antennas are a possible alternative to horns in feed applications or as a feeder for a horn. Multilayer patch antennas can provide a return loss of 10dB or better a 50% or more bandwidth. Microstrip feed antennas are

usually singly or in arrays and can be incorporated in a cavity or a horn to improve the radiation performance for feed applications where low noise temperature is required. Microstripline feeding through various feeding techniques and here centre fed. It is given to ensure that the entire radiation patch is getting equal power distribution. Schematic of the line feed being created and all connected to the radiating element and continuously the ports are been checked for coupling, which energizes transmission and reception. Upon estimating mesh frequencies S parameter simulation frequencies are being set up to get the radiation pattern. The top layer and bottom layer are simulated individually to get the radiation pattern. The parameter analyzed includes polarization and radiation pattern measurements in magnetic plane are made.

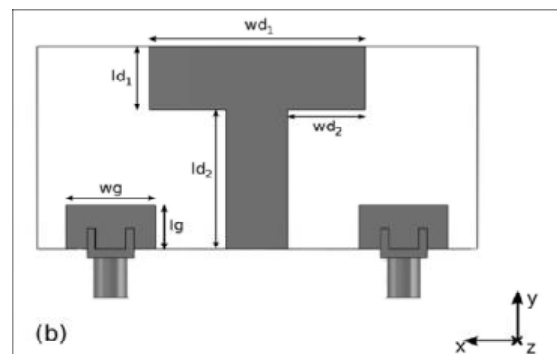
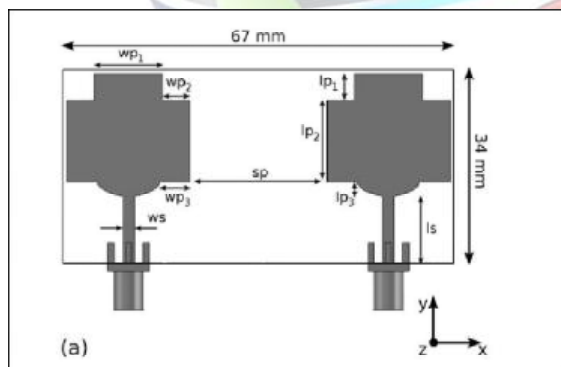


Fig: Layout of antenna structures (a) Top layer layout with transmitting and receiving radiating patches (b) Bottom layers with decoupling structures a partial ground plane. Dimensions $wp1=10\text{mm}$ $wp2=4\text{mm}$, $wp3=4\text{mm}$, $lp1=4\text{mm}$, $lp2=12\text{mm}$, $lp3=2.1\text{mm}$, $ws=1.7\text{mm}$, $ls=9.9\text{mm}$, $sp=20\text{mm}$, $wg=11.5\text{mm}$, $lg=6.25\text{mm}$, $wd1=28\text{mm}$, $wd2=10\text{mm}$, $ld1=9\text{mm}$, $ld2=20\text{mm}$.

D.ARTEFACT-DOMINANT WINDOW SELECTION FOR ADAPTIVE ARTEFACT FILTERING

The proposed artefact removal algorithm combines the best attributes of the Entropy-based Time Window algorithm and the Wiener Filter algorithm. The first step of the proposed artefact removal algorithm is to automatically select the artefact-dominated portion of backscattered signals based on entropy values. In order to better select the artefact window, the proposed algorithm improves upon the original Entropy-based Time Window artifact removal algorithm proposed. While their algorithm is effective in removing the artefact, it often fails to correctly estimate the exact portion of the signal containing the artefact. It also tends to

remove part of tumor response when early-time artifact and tumor responses overlap in time.

Therefore, an improved algorithm was developed by the authors that more accurately estimates the artefact-dominated portion of the signal. The Entropy-based Time Window algorithm is based on the assumption that the artefacts in the received signals are similar across all channels, unlike the case for the tumour response in real breast imaging scenarios (the tumour response is delayed and attenuated differently due to variations in the tissue structures at each channel). A larger value of entropy is obtained from similar artefacts in the early portion of the radar signal, and conversely, the tumour reflections result in a much lower entropy value.

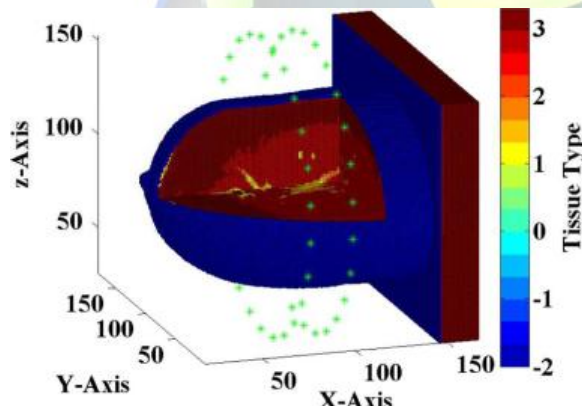


Fig 1. Three-dimensional FDTD breast model and antenna configuration.

III. SIMULATIONS AND PERFORMANCE METRE

An accurate 3-D FDTD model must combine the appropriate geometrical properties of the breast, the heterogeneity, and spatial distribution of the different component tissues within the breast. The FDTD method inherently provides information about the electromagnetic field within the computational volume over the entire period of the simulation. Only a small fraction of this information is used when investigating conventional antenna parameters. The models considered in this study are based on the UWCEN MRI breast cancer repository. The antenna elements are dipped in a coupling medium matching the dielectric properties of adipose tissue. The entire simulation space is 150mm, 150mm, 150mm. Each location within the breast is described in terms of coordinates. For completeness, three breast models have been considered in this study: a homogeneous breast model composed of adipose breast tissues only; a heterogeneous model with heterogeneous adipose tissues; and finally a full heterogeneous model with both heterogeneous adipose and fibro glandular tissues. An 8-mm tumor is placed at different locations within each breast model: a tumor located close to the skin at position (65 mm, 65 mm, 35 mm); at position (88 mm, 65 mm, 45mm); and at (88 mm, 65mm, 100 mm). A 200-ps differentiated Gaussian pulse is transmitted and recorded at each of the 50 antennas. The input pulse has a center frequency of 6.0 GHz and a 3-dB

bandwidth of 5 GHz. FDTD simulations are conducted at a sampling rate of 576 GHz. Prior to any signal processing, all FDTD signals are down-sampled from 576 to 57.6 GHz.

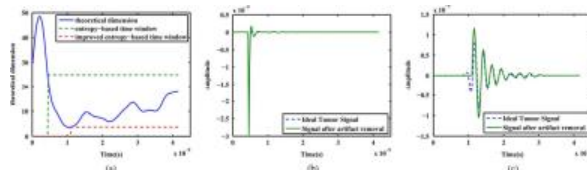


Fig. 2. (a) Theoretical dimension and time window functions. (b), (c) Time-domain signals obtained after multiplying time window functions and corresponding ideal tumor signals. (a) Original time window. (b) Original time window. (c) Improved time window.

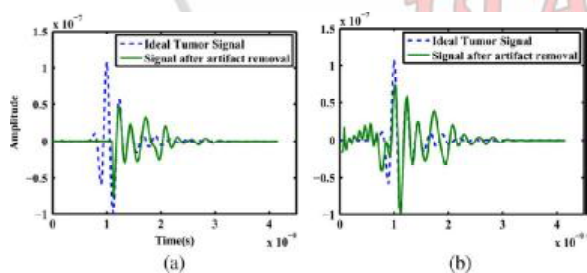


Fig. 3. Time-domain signals after artefact removal. (a) Multiplication with improve time window. (b) Wiener Filter over improved time window.

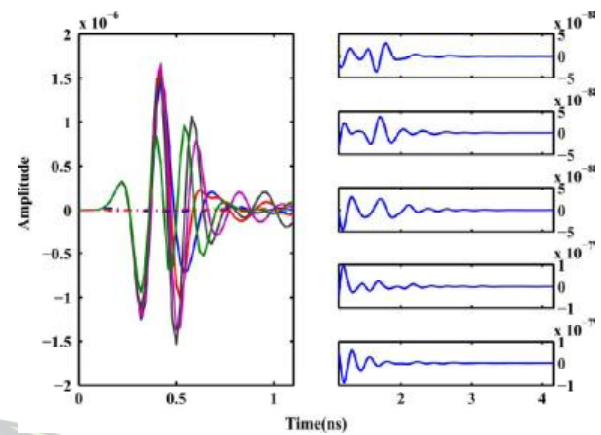


Fig. 4. Time-domain signals before (solid lines) and after (dotted lines) artifact removal using proposed hybrid algorithm at five different channels: (left) earlytime response (artifact) and (right) late-time response (tumor signal) (note different amplitude ranges between early and late-time signals).

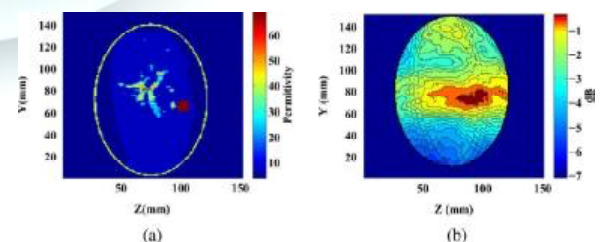


Fig. 5. Coronal view of FDTD breast model showing (a) permittivity of breast tissues computed at 6.0 GHz and (b) corresponding



beamformed image obtained after artifact removal using hybrid algorithm.

IV. CONCLUSION

In this letter, a hybrid artefact removal algorithm for microwave breast imaging applications is presented, which combines the best attributes of two existing algorithms to effectively remove the early-stage artifact while preserving the tumor response. A time window is designed based on the entropy values, which represents the artifact-dominant part of the signal, and the artifact is removed by applying the Wiener Filter algorithm over the estimated artifact window.

After artefact removal, beamformed images are obtained using a simple delay-and-sum beamformer. Results indicate that the proposed algorithm provides for an improved artifact window selection and uses a Wiener Filter to remove the artifact while preserving the tumor response across all channels. The algorithm is compared to the Entropy-based Time Window algorithm, and results indicate that the proposed algorithm performs better in terms of signal and image quality metrics, from simple homogeneous scenarios to more realistic dielectrically heterogeneous scenarios.

Future work will focus on extending the proposed algorithm for artifact removal to the more challenging scenario of multistatic radar signals.

V. REFERENCES

- [1] W. Zhi and F. Chin, "Entropy-based time window for artifact removal in UWB imaging of breast cancer detection," *IEEE Signal Proces.Lett.*, vol. 13, no. 10, pp. 585–588, Oct. 2006.
- [2] E. Bond, X. Li, S.Hagness, and B. VanVeen, "Microwave imaging via space-time beamforming for early detection of breast cancer," *IEEETrans. Antennas Propag.*, vol. 51, no. 8, pp. 1690–1705, Aug. 2003.
- [3] E. J. Bond, X. Li, S. C. Hagness, and B. D. V. Veen, "Microwave imaging via space-time beamforming for early detection of breast cancer," *IEEE Trans. Antennas Propag.*, vol. 51, no. 8, pp. 1690–1705, Aug. 2003.
- [4] E. Zastrow, S. K. Davis, M. Lazebnik, F. Kelcz, B. D. V. Veen, and S. C. Hagness, "Database of 3D grid-based numerical breast phantoms for use in computational electromagnetics simulations,"

Department of Electrical and Computer Engineering, University of



Wisconsin–Madison, Madison, WI, USA, 2008
[Online]. Available:

<http://uwcem.ece.wisc.edu/home.htm>

[5] M. Lazebnik, D. Popovic, L. McCartney, C. B. Watkins, M. J. Lindstrom, J. Harter, S. Sewall, T. Ogilvie, A. Magliocco, T.M. Breslin, W. Temple, D. Mew, J. H. Booske, M. Okoniewski, and S.C. Hagness, “A large-scale study of the ultrawideband microwave dielectric properties of normal, benign and malignant breast tissues obtained from cancer surgeries,” *Phys. Med. Biol.*, vol. 52, pp. 6093–6115, 2007.

[6] X. Li and S. Hagness, “A confocal microwave imaging algorithm for breast cancer detection,” *IEEE Microw. Wireless Compon. Lett.*, vol. 11, no. 3, pp. 130–132, Jul. 2001.

